ChemComm

Chemical Communications

The Effects of Conformation on the Noncovalent Bonding Interactions in a Bistable Donor-Acceptor [3]Catenane

Cheng Wang,[a] Dennis Cao,[a,b] Albert C. Fahrenbach,[a] Sergio Grunder,[a] Sanjeev K. Dey,[a] Amy A. Sarjeant,[a] and J. Fraser Stoddart*[a,b]

[a] *Department of Chemistry, Northwestern University, 2145 Sheridan Road, Evanston, Illinois 60208, United States.*

[b] *NanoCentury KAIST Institute and Graduate School of EEWS (WCU), Korea Advanced Institute of Science and Technology (KAIST)373−1, Guseong Dong, Yuseong Gu, Daejeon 305−701, Republic of Korea.*

SUPPORTING INFORMATION

Table of Contents

1. General Methods

All reagents and starting materials were purchased from Aldrich or VWR and used without further purification. Compounds **3**[S1], **5**[S2], **8**[S3] and 1,1′-[1,4-phenylenebis-(methylene)]-bis(4,4′-bipyridinium) bis(hexafluorophospate)[S4] were prepared according to the literature. All reactions were performed under an argon atmosphere and in dry solvents unless otherwise noted. Column chromatography was carried out using silica gel 60 as the stationary phase. High Performance Liquid Chromatography (HPLC) purification was performed on a preparative reverse phase-HPLC (RP-HPLC) instrument, using a C18 column. UV-Vis spectra were recorded on a Varian 100-Bio UV/Vis spectrophotometer. 1D and 2D nuclear magnetic resonance (NMR) spectra were recorded on Bruker Avance III 500 and 600 MHz spectrometers. Chemical shifts are reported in ppm relative to the signals corresponding to the residual non-deuterated solvent. High resolution electrospray ionization (HR ESI) mass spectra were measured on Agilent 6210 LC-TOF with Agilent 1200 HPLC introduction. High-resolution matrix-assisted laser desorption/ionization (MALDI) mass spectra were measured on a Bruker Autoflex III mass spectrometer. Electrochemical experiments were carried out at room temperature in argon-purged solutions, with a Gamry Reference 600 potential station interfaced to a PC. Cyclic voltammetry and differential pulse voltammetry (DPV) experiments were performed using a glassy carbon working electrode. Its surface was polished routinely with alumina-water slurry on a felt surface immediately before use. The counter electrode was a Pt coil and the reference electrode was a standard Ag/AgCl electrode. The X-ray crystal data for **1**·8PF_6 were collected at 173 K using a Rigaku 007HF RA generator (Mo-K_α radiation) equipped with confocal optics and Saturn 944+ CCD system. The structures were solved by direct methods. CCDC 886394 contains crystallographic data for this paper.

S2. Synthetic Procedures

Scheme S1 Synthesis of compound **4**

Compound 4: Et_3N (1.09 g, 1.50 mL, 10.7 mmol) and *N*,*N*′-dimethylaminopyridine (DMAP) (50 mg) were added to a solution of the compound **3** (985 mg, 1.60 mmol) in dry CH_2Cl_2 (50 mL) at 0 °C under a nitrogen atmosphere. A solution of *p*-toluene-sulfonylchloride (0.92 g, 4.80 mmol) in dry CH_2Cl_2 (20 mL) was added directly to the reaction in 1 h. The reaction mixture was allowed to warm up to room temperature, before being stirred for an additional 11 h. After removing the solvents under reduced pressure, the resulting mixture was purified by column chromatography [SiO_2 : CH_2Cl_2 / MeOH (100 : 1)]. The product ditosylate **4** was isolated as a yellow oil (1.08 g, yield, 72%). ^{1}H NMR ($CDCl_3$, 500 MHz, 298K, ppm): δ = 7.78 (d, *J* = 8.5 Hz, 4H), 7.33 (d, *J* = 8.5 Hz, 4H), 6.21 (s, 2H), 4.27 (s, 4H), 4.14 (t, *J* = 4.5 Hz, 4H), 3.68–3.58 (m, 28H), 2.44 (s, 6H). ^{13}C NMR ($CDCl_3$, 125 MHz, 298K, ppm): δ = 144.9, 134.5, 134.5, 132.9, 129.9, 128.0, 116.5, 116.3, 110.6, 110.5, 70.8, 70.6, 70.6, 70.6, 70.5, 69.3, 69.2, 68.7, 68.2, 68.2, 21.7. MALDI–TOF MS: calcd for $C_{38}H_{52}O_{14}S_6$ *m/z* = 924.168 $[M]^+$, found: *m/z* = 924.164 $[M]^+$.

Scheme S2 Synthesis of compound **6**

Compound 6: Compound **4** (1.84g, 2 mmol), compound **5** (1.68 g, 0.5 mmol), K_2CO_3 (1.10 g, 8 mmol) and LiBr (30 mg) were added to MeCN (80 mL). The reaction mixture was heated under reflux under argon for 12 h. After cooling down to the room temperature and removing the solvents under reduced pressure, the resulting mixture was purified by column chromatography [SiO_2 : EtOAc / CH_2Cl_2 / MeOH (6: 6: 1)]. The diol **6** was isolated as a yellow oil (1.62 g, yield, 65%). ^{1}H NMR ($CDCl_3$, 500 MHz, 298K, ppm): δ = 7.85 (d, *J* = 8.5 Hz, 4H), 7.33 (t, *J* = 8.0 Hz, 4H), 6.83 (d, *J* = 7.5 Hz, 4H), 6.16 (s, 1H), 6.15 (s, 1H), 4.30–4.27 (m, 8H), 4.22 (s, 4H), 3.99 (t, *J* = 5.0 Hz, 8H), 3.81–3.78 (m, 8H), 3.71–3.55 (m, 40H). ^{13}C NMR ($CDCl_3$, 125 MHz, 298K, ppm): δ = 154.4, 154.4, 130.6, 130.5, 126.8, 126.8, 125.2, 116.5, 116.4, 114.7, 114.6, 110.6, 110.6, 105.7, 105.7, 72.6, 71.1, 71.1, 70.8, 70.8, 70.7, 70.4, 69.9, 69.9, 69.3, 68.3, 68.3, 68.0, 61.8. MALDI–TOF MS: calcd for $C_{60}H_{84}O_{20}S_4$ *m/z* = 1252.444 $[M]^+$, 1275.434 $[M+Na]^+$,; found: *m/z* = 1252.296 $[M]^+$, 1275.290 $[M+Na]^+$.

Scheme S3 Synthesis of compound **7**

Compound 7: Et_3N (1.09 g, 10.7 mmol), compound **6** (1.25 g, 1.0 mmol) and *N*, *N*′-dimethylaminopyridine (DMAP) (20 mg) were added to dry CH_2Cl_2 (100 mL) at 0 °C. A solution of *p*-toluene-sulfonylchloride (0.76 g, 4.0 mmol) in dry CH_2Cl_2 (20 mL) was added directly to the reaction mixture during 1 h under a nitrogen atmosphere. It was allowed to warm up to room temperature, before being stirred for an additional 2 h. After removing the solvents under reduced pressure, the resulting mixture was purified by column chromatography [SiO_2 : CH_2Cl_2 / EtOAc (1 : 2)]. The product ditosylate **7** was isolated as a yellow oil (1.22 g, yield, 78%). ^{1}H NMR (CD_2Cl_2, 500 MHz, 298K, ppm): δ = 7.83 (t, *J* = 7.5 Hz, 4H), 7.76 (d, *J* = 8.5 Hz, 4H), 7.37–7.34 (m, 8H), 6.86 (m, 4H), 6.22 (s, 1H), 6.21 (s, 1H), 4.29–4.26 (m, 8H), 4.23 (s, 4H), 4.10–4.08 (m, 4H), 3.97–3.94 (m, 8H), 3.76–3.72 (m, 8H), 3.66–3.51 (m, 36H), 2.41 (s, 6H). ^{13}C NMR (CD_2Cl_2, 125 MHz, 298K, ppm): δ = 154.8, 154.7, 145.5, 135.0, 135.0, 133.2, 130.3, 128.3, 127.0, 127.0, 125.6, 116.8, 116.7, 114.8, 114.7, 110.8, 106.0, 71.3, 71.3, 71.0, 71.0, 71.0, 71.0, 70.8, 70.1, 69.9, 69.8, 69.0, 68.5, 68.4, 68.4, 21.8. MALDI–TOF MS: calcd for $C_{74}H_{96}O_{24}S_6$ *m/z* = 1560.462 $[M]^+$; found: *m/z* = 1559.935 $[M]^+$.

Scheme S4 Synthesis of compound **2**

Compound 2: NaH (0.14 g, 6.0 mmol) was suspended in dry, degassed THF (400 mL) and a mixture of the compound **7** (1.09 g, 0.7 mmol), compound **8** (0.19 g, 0.7 mmol) and Cs_2CO_3 (0.33 g, 1 mmol) in dry, degassed THF (40 mL) was added with syringe pump during 24 h while refluxing under Argon. After stirring and refluxing for a further 3 d, the reaction mixture was cooled down to room temperature, and MeOH (20 mL) was added very carefully. The solvents were removed under vacuum, and the residue extracted into CH_2Cl_2 (250 mL). The organic layers were washed with H_2O (2 × 30 mL), before being dried ($MgSO_4$) and concentrated under reduced pressure to afford a residue which was subjected to column chromatography [SiO_2 : EtOAc / CH_2Cl_2 / MeOH (50: 50: 1)]. The macrocyclic polyether **2** was isolated as a yellow oil (0.27 g, yield, 26%). ^{1}H NMR ($CDCl_3$, 500 MHz, 298K, ppm): δ = 7.85 (d, *J* = 8.5 Hz, 4H), 7.33 (t, *J* = 8.0 Hz, 4H), 6.83 (d, *J* = 7.5 Hz, 4H), 6.14 (s, 2H), 6.12 (s, 2H), 4.30–4.25 (m, 8H), 4.19 (s, 4H), 4.18 (s, 4H), 4.00–3.96 (m, 8H), 3.80–3.76 (m, 8H), 3.70–3.51 (m, 40H). ^{13}C NMR ($CDCl_3$, 125 MHz, 298K, ppm): δ = 154.4, 134.7, 134.5, 126.8, 125.3, 116.5, 116.4, 114.7, 110.6, 105.8, 71.1, 70.8, 70.8, 70.8, 70.7, 69.9, 69.3, 69.3, 68.3, 68.2, 68.0. HR MS (ESI): Calcd for $C_{68}H_{88}O_{20}S_8$ *m/z* = 1481.3707 $[M + H]^+$, 1498.4007 $[M + NH_4]^+$, found *m/z* = 1481.3699 $[M + H]^+$, 1498.4001 $[M + NH_4]^+$.

Scheme S5 Synthesis of compound **1**·8PF_6

1·8PF_6: A mixture of ′4,4 -bis(bromomethyl)benzene (69 mg, 0.20 mmol), the macrocyclic polyether **2** (73 mg, 0.05 mmol), and 1,1′-[1,4-phenylenebis(methylene)]-bis(4,4′-bipyridinium) bis(hexafluorophospate) (0.14 g, 0.20 mmol) were dissolved in DMF (10 mL). The reaction mixture was subjected to 15 kbar in an ultra high pressure reaction chamber at room temperature for 5 d. After removing the solvents under reduced pressure, the resulting mixture was purified by RP-HPLC (water-MeCN 0-60% in 20 min, λ = 254 nm) to yield **1**·8PF_6 as a green solid (65 mg, 35 %) after counterion exchange with NH_4PF_6. ^{1}H NMR ($CDCl_3$, 500 MHz, 298K, ppm): δ = 9.02–8.48 (m, 16H), 8.03–7.82 (m, 5H), 7.64–7.06 (m, 34H), 6.77–6.61 (m, 3H), 6.22–6.04 (m, 3H), 5.95–5.83 (m, 3H), 5.77–5.44 (m, 16H), 4.28–3.45 (m, 72H). HR MS (ESI): Calcd for $C_{140}H_{152}F_{48}N_8O_{20}P_8S_8$ *m*/*z* = 1695.3364 $[M - 2PF_6]^{2+}$, 1081.9027 $[M - 3PF_6]^{3+}$, found *m*/*z* = 1081.9025 $[M - 2PF_6]^{2+}$, 1695.3352 $[M - 3PF_6]^{3+}$.

S3. X-Ray Crystallography

Data Collection for 1·8PF$_6$: A dark green block crystal of $C_{140}H_{152}N_8O_{20}F_{48}P_8S_8$, having the approximate dimensions of 0.093 × 0.044 × 0.038 mm, was mounted using oil (Infineum V8512) on a glass fiber. All measurements were made on a CCD area detector with CuKα microsource equipped with MX optics.

Cell parameters and an orientation matrix for data collection corresponded to a monoclinic cell with dimensions:

a = 13.9148(6) Å α = 93.109(4)°

b = 16.0786(8) Å β = 104.124(3)°

c = 21.8368(11) Å γ = 90.629(3)°

V = 4729.4(4) Å^3

For Z = 1 and F.W. = 3682.94, the calculated density is 1.564 g·cm^{-3}. Based on a statistical analysis of intensity distribution, and the successful solution and refinement of the structure, the space group was determined to be *P*-1. The data was collected at a temperature of 100(2)K with a θ range for the data collection of 4.18 to 125.12º. 22595 reflections measured, 14503 unique (R_{int} = 0.0955) which were used in all calculations. The final $wR(F_2)$ was 0.3540 (all data). Global rigid bond restraints (esd 0.01) were imposed on the displacement parameters as well as restraints on similar amplitudes (esd 0.04) separated by less than 1.7Å.

One PF_6^- counterion is disordered over two crystallographically unique positions. The counterion including P5 was subjected to a SAME restraint linking it to the counterion containing P1. Additionally, a SAME restraint was used to link the two halves of the larger macrocycle. The solvent masking procedure as implemented by Olex2 was used to remove electronic contributions from disordered solvent. Total solvent accessible volume / cell = 973.1 Å^3 [20.6%]. Total electron count / cell = 191.9. As the exact content of the solvents disordered in the lattice is not known, only the atoms used in the refinement model are reported in the formula given here.

Table S1. Crystal Data and Structure Refinement for **1**·8PF_6

Empirical formula	$C_{140}H_{152}N_8O_{20}F_{48}P_8S_8$
Formula weight	3682.94
Temperature	100(2) K
Wavelength	1.54178 Å
Crystal system, space group	triclinic, *P*-1
Unit cell dimensions	a = 13.9148(6) Å, α = 93.109(4)°
	b = 16.0786(8) Å, β = 104.124(3)°
	c = 21.8368(11) Å, γ = 90.629(3)°
Volume, V	4729.4(4)Å^3
Z, Calculated density	1, 1.293 g·cm^{-3}
Absorption coefficient	2.428 mm^{-1}
F(000)	1888
Crystal size	0.093 × 0.044 × 0.038 mm
Theta range for data collection	4.18 to 125.12º
Limiting indices	$-9\leq h\leq 15$, $-18\leq k\leq 18$, $-25\leq l\leq 25$
Reflections collected / unique	22595 / 14503 [R_{int} = 0.0955]
Data / restraints / parameters	14503/1128/1109
Goodness-of-fit on F^2	1.052
Final R indices [$I > 2\sigma(I)$]	R_1 = 0.1280, wR_2 = 0.3112
R indices (all data)	R_1 = 0.2774, wR_2 = 0.3540
Largest diff. peak and hole	+0.585 and –0.406 e·Å^{-3}

S4. UV/Vis Absorption Spectroscopic Characterization

In the UV-Vis experiments, $Fe(ClO_4)_3$ was used as an oxidant in MeCN solution at room temperature. After addition of $Fe(ClO_4)_3$ to the solution of macrocyle **1**, two new major peaks with λ_{max} = 540 nm and 800 nm besides the characteristic absorption band of $TTF^{\bullet+}$ radical (430 nm and 600 nm) were detected. In common with previous results,[S5] these two peaks should be assigned to the characteristic absorption band of $TTF^{+\cdot}$ radical dimer in macrocyclic polyether **2**. Their intensities reach its maximum at 2 equiv of $Fe(ClO_4)_3$. Further addition of $Fe(ClO_4)_3$ will decrease the intensity of those peaks. After full oxidation of TTF (addition for 4 to 5 equiv. of $Fe(ClO_4)_3$), however, a broad peak centered at 800 nm still exists. We assume that this peak can be ascribed to the CT band between the electron deficient TTF^{2+} and electron efficient DNP.

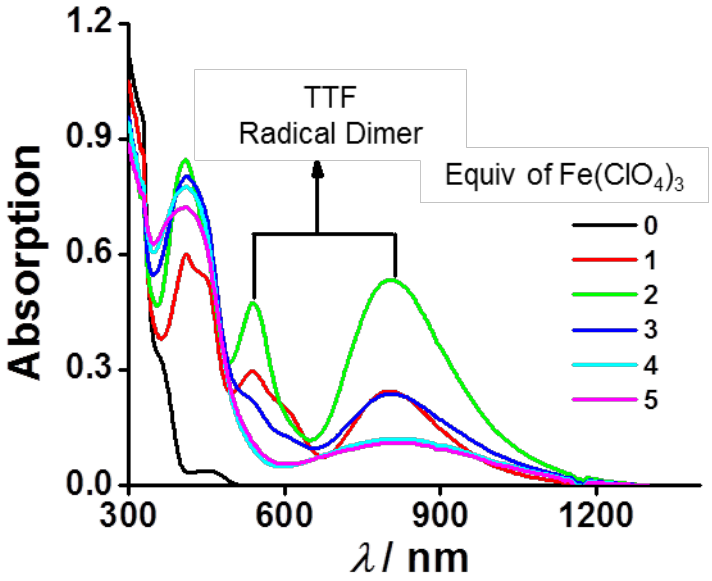

Fig. S1 Absorption spectra of the macrocyclic polyether **2** (5.0×10^{-5} M, MeCN, 10 mm path length, 298 K) recorded upon addition of up to 4.0 equiv. of $Fe(ClO_4)_3$.

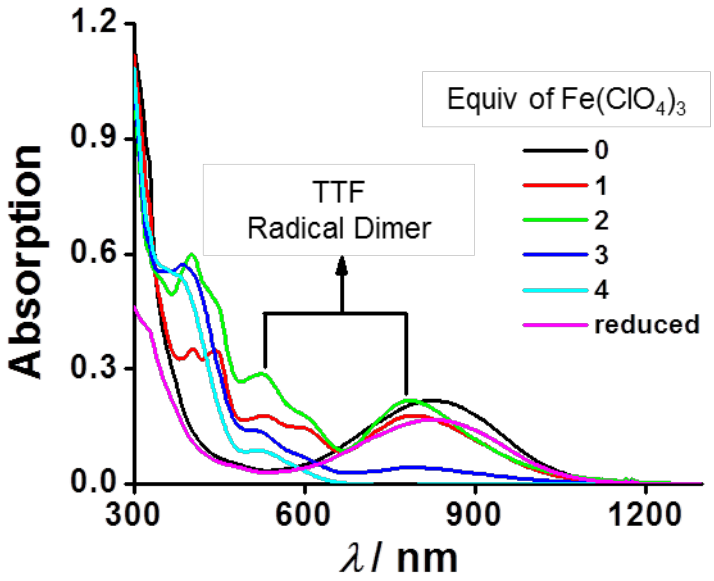

Fig. S2 Absorption spectra (MeCN, 298 K) of a 5.0×10^{-5} M solution of **1**·8PF_6 and of the same solution after addition of 1.0, 2.0, 3.0 and 4.0 equiv of $Fe(ClO_4)_3$. Addition of 2.5 equiv of ascorbic acid gives back the original spectrum.

The formation of TTF radical cation dimer in **1**·8PF_6 was also investigated by UV-Vis spectroscopy. After addition of $Fe(ClO_4)_3$ (up to 2 equiv), besides an increase in the intensity of the absorption bands of $TTF^{+\cdot}$ at 450 and 600 nm, another two absorption bands centered on 523 and 785 nm also appeared. They can be assigned to the characteristic absorption band of the TTF radical cation dimer. The intensities of these bands arising from dimierization are approximately half of those observed for the free macrocyclic polyether **2** under identical conditions, leading us to estimate that the equilibrium ratio between $TTF^{\cdot+}$ radical cation dimer and monomer to be about 1:1 in the $\mathbf{1}^{4+2(\cdot+)}$ catenane. The ability to dimerize in the catenane is hindered by the energetic cost of bringing the bulky and positively charged $CBPQT^{4+}$ rings closer together.

S5. Electrochemical Behavior

Cyclic voltammetry (CV) and differential pulse voltammetry (DPV) experiments were performed in a Gamry Reference 600 potential station. Fig. S3 shows the CV spectrum of macrocyclic polyether **2**. The first and second oxidation peaks were found around +0.34 and +0.81 V. The first peak was shifted to the lowering potentials as a result of the formation of TTF radical cation dimers. In the CV experiment (Fig. S4) of **1**·8PF_6, the first oxidation peak of TTF which is around +0.50 V for 'free' TTF is hardly detectable at all in the anodic scan. DPV analysis shows (Fig. S5) a small peak around +0.46 V. These resulsts indicate the existence of some 'free' TTF in association with a small amount of the minor translational isomer present in **1**·8PF_6 at equilibrium. In the reduction region, three redox process whose peaks were observed at were found around –0.32, –0.43 and –0.82 V, corresponding to a one-, one-, and two- electron reduction, respectively.

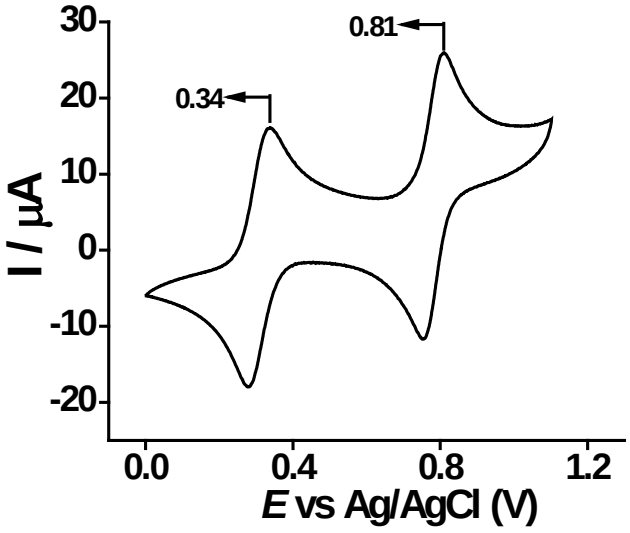

Fig. S3 The CV of macrocyclic polyether **2**. The data were recorded in Ar-purged MeCN at 298 K. The concentrations of the sample and supporting electrolyte were 1 mM and 0.1 M, respectively.

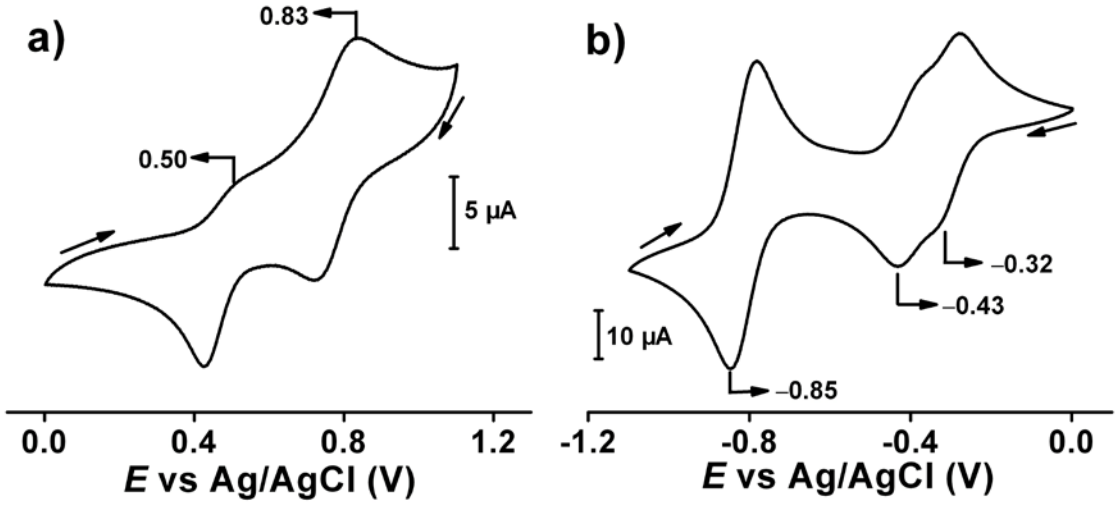

Fig. S4 Cyclic voltammetric curves of **1**·8PF_6 recorded in the (a) oxidation region and (b) the reduction region. The concentrations of the sample and supporting electrolyte were 0.5 mM and 0.1 M, respectively.

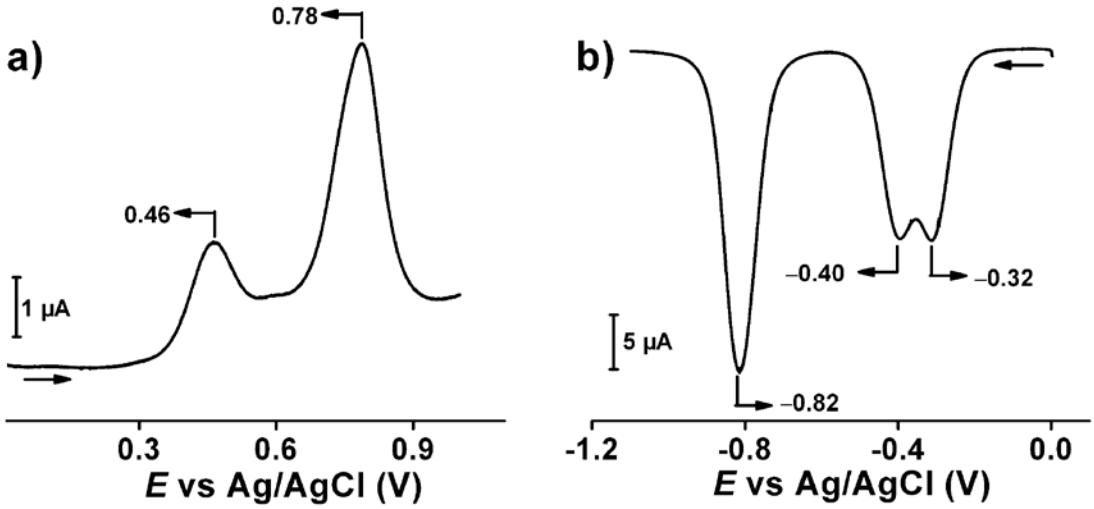

Fig. S5 DPV of **1**·8PF_6 in (a) oxidation and (b) reduction processes. The data were recorded in Ar-purged MeCN at 298 K. The concentrations of the sample and supporting electrolyte were 0.5 mM and 0.1 M, respectively.

S6. ^{1}H NMR Spectroscopy

The chemical switching behavior of $\mathbf{1}^{8+}$ was monitored (Fig. S6) by ^{1}H NMR spectroscopy in CD_3CN at 233 K. The NMR resonances were assigned based on ^{1}H-^{1}H gradient-selected double-quantum-filtered correlation spectroscopy (^{1}H-^{1}H-g-DQF-COSY). In the ground state, the ^{1}H NMR spectrum of $\mathbf{1}^{8+}$ is quite complicated, and as a sequence, even from the ^{1}H-^{1}H-g-DQF-COSY spectrum, peak assignments are difficult. After addition of tris(4-bromophenyl)aminium hexachloroantimonate, however, the ^{1}H NMR spectrum became very simple and the peaks can be assigned with the assistance of the ^{1}H-^{1}H-g-DQF-COSY spectrum (Fig. S7).

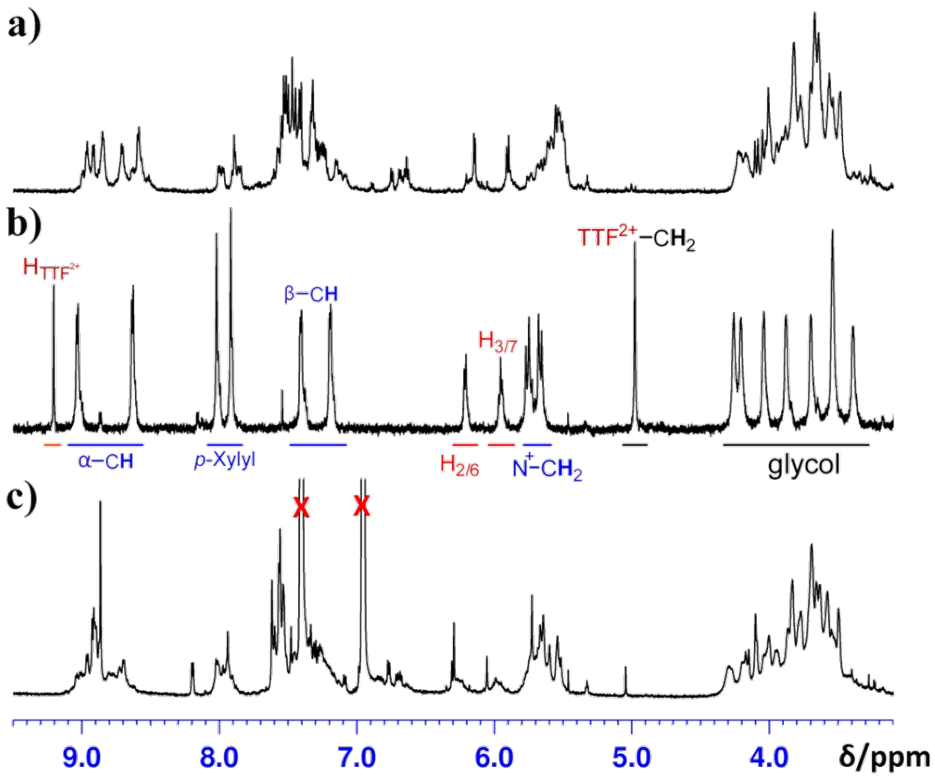

Fig. S6 ^{1}H NMR spectra (600 MHz, 233 K, CD_3CN) of a) **1**·8PF_6; b) Following oxidation with 6.0 equiv tris(4-bromophenyl)aminium hexachloroantimonate; c) Following reduction with Zn dust.

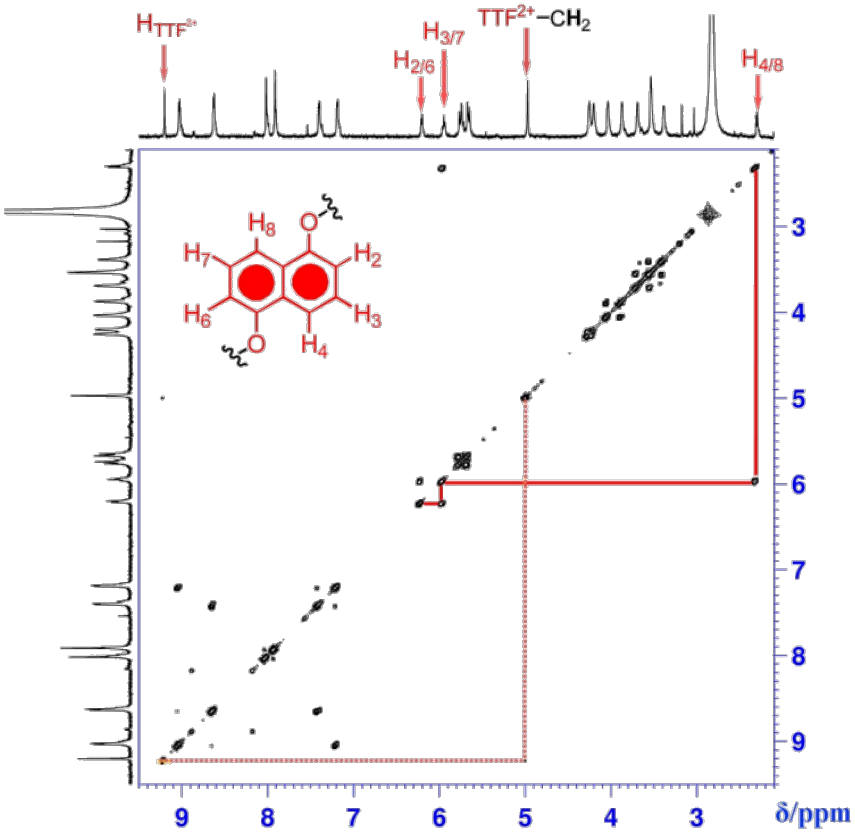

Fig. S7 ^{1}H-^{1}H-g-DQF-COSY spectrum of **1**·8PF_6 after addition of tris(4-bromophenyl)aminium hexachloroantimonate in CD_3CN at 233 K, recorded on a 600 MHz spectrometer.

S7. References

S1. M. Asakawa, P. R. Ashton, V. Balzani, A. Credi, G. Mattersteig, O. A. Matthews, M. Montalti, N. Spencer, J. F. Stoddart and M. Venturi, *Chem. Eur. J.*, 1997, **3**, 1992–1996.

S2. S. Basu, A. Coskun, D. C. Friedman, M. A. Olson, D. Benítez, E. Tkatchouk, G. Barin, J. Yang, A. C. Fahrenbach, W. A. Goddard and J. F. Stoddart, *Chem. Eur. J.*, 2011, **17**, 2107–2119.

S3. R. Andreu, J. Garín, J. Orduna, M. SaviroÂ n, J. Cousseau, A. Gorgues, V. Morisson, T. Nozdryn, J. Becher, R. P. Clausen, M. R. Bryce, P. J. Skabara and W. Dehaen, *Tetrahedron Lett.*, 1994, **35**, 9243–9246.

S4. P. R. Ashton, J. Huff, S. Menzer, I. W. Parsons, J. A. Preece, J. F. Stoddart, M. S. Tolley, A. J. P. White and D. J. Williams, *Chem. Eur. J.*, 1996, **2**, 31−44.

S5. A. Coskun, J. M. Spruell, G. Barin, A. C. Fahrenbach, R. S. Forgan, M. T. Colvin, R. Carmielli, D. Benítez, E. Tkatchouk, D. C. Friedman, A. A. Sarjeant, M. R. Wasielewski, W. A. Goddard III and J. F. Stoddart, *J. Am. Chem. Soc.*, 2011, **133**, 4538−4547.